

Quantized biopolymer translocation through nanopores: Departure from simple scaling

Simone Melchionna,^{1,2} Massimo Bernaschi,³ Maria Fyta,^{1,*} Efthimios Kaxiras,^{1,4} and Sauro Succi^{3,4}

¹*Department of Physics and School of Engineering and Applied Sciences, Harvard University,
17 Oxford Street, Cambridge, Massachusetts 02138, USA*

²*INFN-SOFT, Department of Physics, Università di Roma "La Sapienza," P. le A. Moro 2, 00185 Rome, Italy*

³*Istituto Applicazioni Calcolo, CNR, Viale del Policlinico 137, 00161 Rome, Italy*

⁴*Initiative in Innovative Computing, Harvard University, Cambridge, Massachusetts 02138, USA*

(Received 3 December 2008; published 3 March 2009)

We discuss multiscale simulations of long biopolymer translocation through wide nanopores that can accommodate multiple polymer strands. The simulations provide clear evidence of folding quantization, namely the translocation proceeds through multifolded configurations characterized by a well-defined integer number of folds. As a consequence, the translocation time acquires a dependence on the average folding number, which results in a deviation from the single-exponent power law characterizing single-file translocation through narrow pores. The mechanism of folding quantization allows polymers above a threshold length (approximately 1000 persistence lengths for double-stranded DNA) to exhibit cooperative behavior, and as a result to translocate noticeably faster.

DOI: [10.1103/PhysRevE.79.030901](https://doi.org/10.1103/PhysRevE.79.030901)

PACS number(s): 82.35.Pq, 47.11.St

The translocation of biopolymers through nanopores is drawing increasing attention because of its role in many fundamental biological processes, such as viral infection by phages, interbacterial DNA transduction, or gene therapy [1]. This problem has motivated a number of *in vitro* experimental studies, aimed at exploring the translocation process through protein channels across cellular membranes [2,3], or through microfabricated channels [4]. Recent experimental work has addressed the possibility of ultrafast DNA sequencing using electronic identification of DNA bases, while tracking its motion through nanopores under the effect of a localized electric field [5]. Experiments also reported that the translocation of biopolymers through pores wide enough to accommodate multiple strands exhibits the intriguing phenomenon of current-blockade quantization, that is, discrete jumps of the electric current through the pore during the translocation process [6]. This was interpreted as indirect evidence that the polymer crosses the pore in the form of discrete configurations, associated with integer values of the *folding number*, that is, the number of strands simultaneously occupying the pore during the translocation. This behavior was recently confirmed by direct observation of multifolded configurations in large-scale simulations of biopolymer translocation [7].

In the present work, we report on the behavior of long polymers undergoing translocation through relatively wide pores, which exhibits qualitatively unique features. Under these conditions, we predict from our simulations that folding quantization is actually *enhanced* and leads to faster translocation by effectively reducing friction through the pore region. The observed behavior also elicits an intriguing analogy with quantum systems, whereby the observed translocation time can be formulated as a weighted average over the whole set of multifolded configurations (the “pure states”

of the polymer-pore system). Within this picture, the translocation time acquires an additional dependence on the polymer length, through the average value of the folding number $\langle q \rangle_N$, which increases with the polymer length N . Thus, at variance with the case of narrow and short pores [8–12], translocation through wide pores allowing for multiple simultaneous strands is not described by a single power-law exponent. To give a specific example of scales involved, the size of the pores required to observe this behavior in double-stranded DNA is of the order of several (~ 10) times the *effective* cross-sectional diameter (which depends on salt concentration and repulsion between pairs of aligned DNA molecules), while the length threshold above which this behavior emerges is $\sim 150\,000$ base pairs (BPs). What is remarkable and counterintuitive about this behavior is, first, a highly ordered organization of the multiple strands at high folding number, and second, the ability of the quantized configurations to flow through the wide pore without experiencing any additional drag, compared to the single-file configuration.

MULTISCALE MODEL

Our results are obtained from a multiscale treatment of translocation, involving a coarse-grained model for the biopolymer in which the basic unit (“bead”) is equivalent to one persistence length (~ 50 nm), and the molecular motion is coupled to the motion of the solvent in which the biopolymer exists. Incidentally, the length of polymers considered here, up to 8000 beads (equivalent to $\sim 1.2 \times 10^6$ DNA BPs), is an order of magnitude above any previous simulation in the field.

The model couples microscopic molecular dynamics (MD) for the biopolymer bead motion to a mesoscopic lattice Boltzmann (LB) [13] treatment of the solvent degrees of freedom [10]. In contrast to Brownian dynamics, the LB approach handles the fluid-mediated solvent-solvent interactions through an effective representation of local collisions

*Present address: Department of Physics, Technical University of Munich, Germany.

between the solvent and solute molecules. The biopolymer translocates through a nanopore under the effect of a strong localized electric field applied across the pore ends, similar to the conditions in experimental settings [9], with the entire process taking place in the *fast* translocation regime.

A periodic box of size $N_x N_y N_z (\Delta x)^3$ lattice units, with Δx the spacing between lattice points, contains both the solvent and the polymer. All parameters are measured in units of the LB time step and spacing, Δt and Δx , respectively (both set to 1); the MD time step is 0.2. We take $N_x = N_y = N_z$ with the wall at $x = (N_x/2)$, $N_x = 128$, and the number of beads N in the 100–8000 range. At $t=0$, the polymer resides on one side of the separating wall, $x > (N_x/2)$, near the opening of a cylindrical pore of nominal length $l_p = 3$ and nominal diameter d_p ; we considered a narrower, $d_p = 5$, pore and a wider one, $d_p = 9$. Translocation is induced by a constant electric field acting along the x direction and confined to a cylindrical channel of the same size as the pore, and length 3 along the streamwise (x) direction. The pulling force associated with the electric field, E , in the experiments is $q_e E = 0.02$ and the average thermal speed $k_B T / m = 10^{-4}$, where q_e is the effective charge per bead. The interactions between monomers and with the wall are modeled by 6–12 Lennard-Jones potentials [14], and other aspects of the simulation are the same as those in our previous work [10], which successfully reproduced single-file translocation [12,15]. The effective width and radius of the surrounding pore must take into account the repulsive bead-wall interactions that result in an effective exclusion distance of ≈ 1.5 [10]. Therefore, a monomer is considered to lie inside the pore if contained in a pore of effective width $l^{\text{eff}} \approx 6$ (due to exclusion on both sides of the separating wall) and diameter $d^{\text{eff}} \approx 7.5$ for $d_p = 9$ ($d^{\text{eff}} \approx 3.5$ for $d_p = 5$). To measure the residence number of beads in the pore region, we define a cylinder of length $h_p = 10$ and radius d_p centered at the pore midpoint and with axis aligned with the pore. This extended region misses monomers close to the pore openings and in contact with the wall, but permits us to measure the number of beads in a wider region than the pore width with better statistics (reduced variation in the resident-bead number).

CONFIGURATIONAL ANALYSIS—QUANTIZATION OF THE FOLDING NUMBER

In Fig. 1, we show the cumulative statistics of the folding number, $q = N_{\text{res}} / N_1$, collected at each time step of every single trajectory for a series of 100 realizations for each polymer length. Here, N_{res} is the number of resident beads at each given time for each realization, while N_1 is the observed single-file value of the resident number, $N_1 = h_p / b^{\text{eff}} \equiv h_p (1/b + 1/\sigma_b) / 2 \sim 7$ (for values of σ_b and b , see [14,15]). The combined statistics over initial conditions and time evolution produces an aggregate ensemble, ranging from about 10^5 time frames for the shortest history ($N = 100$, $d_p = 9$) up to over 10^7 time frames for the longest one ($N = 8000$, $d_p = 5$). The $d_p = 9$ case reveals a sharp quantization of the distribution of the folding number, with well-defined peaks, which closely resembles the one observed in double-strand DNA translocation through solid nanopores (see Fig. 7 of [16]).

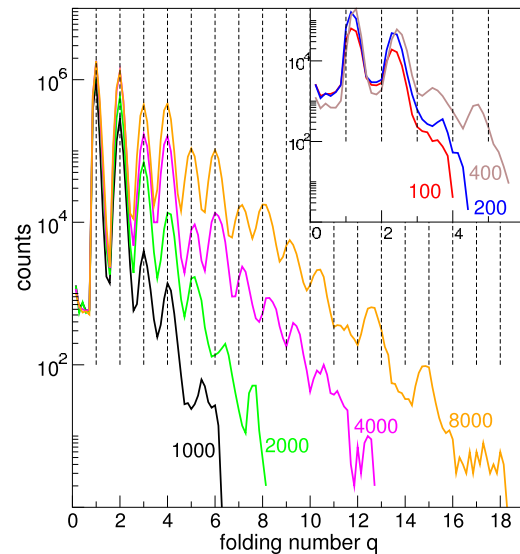


FIG. 1. (Color online) Probability distribution of the folding number q for polymer lengths $N = 1000$ – 8000 and pore width $d_p = 9$. Peaks at integer q values (shown by vertical dashed lines) are evident. The inset shows data for $N = 100$ – 400 at low- q values.

For the shortest strands, $N = 100, 200$, and 400 , the peaks are shifted to values slightly larger than the integer values $q = 1, 2$. This indicates that the polymer spends most of its time between the low-fold states $q = 1, 2$. However, for longer strands $N > 1000$, the peaks of the distribution appear almost perfectly centered at integer values, up to $q = 4, 5$, and 6 , respectively. This quantized spectrum is particularly evident for the case of the longest polymers, $N = 4000$ and 8000 . In this case, “quantum states” up to $q = 10$ are populated, with a slight shift of the peaks to values higher than integer values only for $q > 7$. Note that the quantization is evident up to $q = 10$, which is still significantly smaller than the largest folding number compatible with the pore diameter, $q_{\text{max}} = (d_p / \sigma)^2 \sim 20$ [17]. The value of q above which the quantization gradually diverges from integer values is an increasing function of the polymer length. The $d_p = 5$ case (not presented) shows the same structure, though on a smaller range of q values, up to $q = 5$.

These data suggest an intriguing analogy with quantum systems, the folding number playing the role of the quantum numbers associated with excited states of atomic and molecular configurations. Within this analogy, single-file translocation ($q = 1$) would represent the analog of the ground state of the polymer-pore system. Indeed, the long-term, final stage of the translocation is always found to proceed in single-file mode, corresponding to the polymer tail. In this respect, long polymers translocating through wide pores are naturally expected to exhibit a richer spectrum of excitations versus short polymers translocating through narrow pores. In particular, the number of excited states supported by the polymer-pore system should grow quadratically with the pore diameter. Specifically, a polymer of length $L = bN$ translocating through a pore of length l_p^{eff} and diameter d_p^{eff} can produce a spectrum of folding numbers up to a maximum of $q_{\text{max}} \propto (d_p^{\text{eff}} / \sigma_b)^2$ strands (full-packing limit), each consisting of $N_1 = l_p^{\text{eff}} / b^{\text{eff}}$ monomers. This limit can only be saturated by

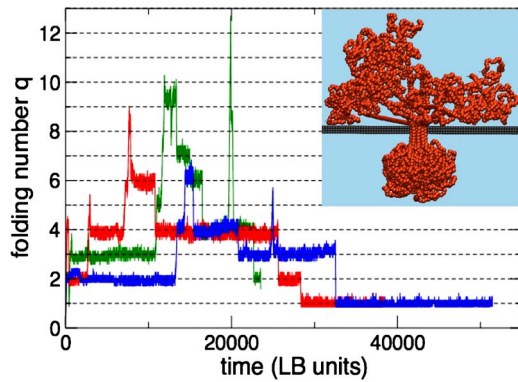


FIG. 2. (Color online) Three trajectories of the folding number sampled from the ensemble $N=4000$ and $d_p=9$. Low- q configurations are most often visited, but $q \geq 10$ can also occur occasionally. The inset shows an actual translocation event at the midpoint with $q=9$.

sufficiently long polymers, such that $N/N_1 \gg q_{\max}$, namely $N \gg N_p \sim l_p^{\text{eff}}(d_p^{\text{eff}})^2/b\sigma_b^2$, with $N_p \sim 100$ the saturation length in the present work.

The statistical picture presented above is supported by the dynamic trajectories. In Fig. 2, we show the time evolution of the folding number $q(t)$ for three histories drawn at random from the pool of 100 realizations of the $N=4000$ system. A very rich dynamics, with sudden jumps between the various “excited states,” is clearly visible. Interestingly, jumps occur both ways, from low to high q and vice versa, corresponding to absorption or emission of “fold quanta.” This indicates that translocation is not monotonic, but consists of a mixed sequence of folding and unfolding events. As anticipated, this sequence is always found to end up in single-file configuration, corresponding to the translocation of the polymer tail. Interestingly, the trajectories spend virtually all of their time in quantized states with very sharp transitions between them. A snapshot of such a quantized state for a highly folded configuration ($q=9$) is shown in the inset of Fig. 2.

SCALING EXPONENTS

In Fig. 3, we report the translocation time as a function of the polymer length, N , for translocation through the wide pore ($d_p=9$). The most probable time from the time distributions, together with the average and the range between the minimum and maximum times, is presented. From this figure, it is apparent that up to a length $N=1000$, the translocation time τ obeys a scaling law of the form $\tau \sim N^\alpha$, with $\alpha \sim 1.36$ for the most probable translocation time, slightly larger than the corresponding value for narrow pores [8–12]. We emphasize that, regardless of the exact values of the scaling exponents, all translocation indicators, that is, the minimum, maximum, most probable, and average translocation times, point clearly toward a deviation from a single-exponent power law in the region $N > 1000$, a clear signature of multifold translocation. By restricting the analysis to the four longest chains, $N=1000, 2000, 4000$, and 8000 , the bending of the curve (reduced translocation time) might be

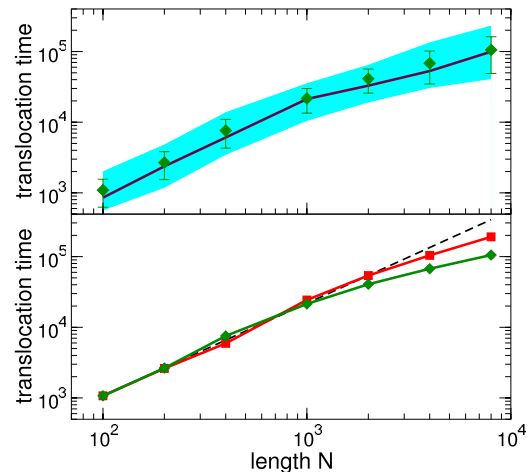


FIG. 3. (Color online) Translocation times as a function of the polymer length (N) for wide pore ($d_p=9$). Top panel shows the average translocation time (green diamonds with associated error bars), the most probable translocation time (solid purple line), and the range between the maximum and minimum translocation times (shaded region). Bottom panel shows a linear fit to the low range results $10^2 < N < 10^3$ (dashed line), the multifile translocation time $\tau_{\text{mf}}(N)$ from Eq. (2) (red squares), and the average translocation time (green diamonds).

interpreted as the emergence of a new scaling exponent, $\alpha_2 \sim 0.75$. However, as shown below, this bending is due to the multifold conformation of the translocating biopolymer, which does not necessarily follow a power-law dependence on the polymer size.

The translocation dynamics depends on the strength of the frictional forces exerted by the wall. In the single-file scenario, strong friction can change the power-law exponent from ≈ 1.2 to a linear relation $\tau \propto N$ [18]. In the case of multifold translocation, a central issue is whether the highly folded configurations induce high-friction conditions. As demonstrated in Fig. 4, dN/dt is linearly correlated to q , with approximately the same slope for all folds. If friction were dominant, dN/dt versus q would asymptotically reach a constant value with increasing q , which is clearly *not* observed in the simulations. Moreover, the dN/dt versus q slope depends only slightly on the polymer length (data not shown), changing by $\sim 30\%$ in going from $N=400$ to 8000 , which is further evidence in support of hydrodynamic coherence inside the pore. It is likely that such coherence arises from small velocity differences between neighboring beads in the pore, by minimizing bead-bead frictional forces, and/or the lubricating effect of the surrounding solvent enhanced by the alignment of strands. Therefore, frictional forces have a negligible effect, possibly limited to a small layer close to the wall, and unimportant for the group of translocating monomers. This rules out the possibility that the change of exponent is caused by frictional forces inside the pore.

Regardless of the underlying nature of the translocation process, we can compute the translocation time of each realization, with τ the total translocation time,

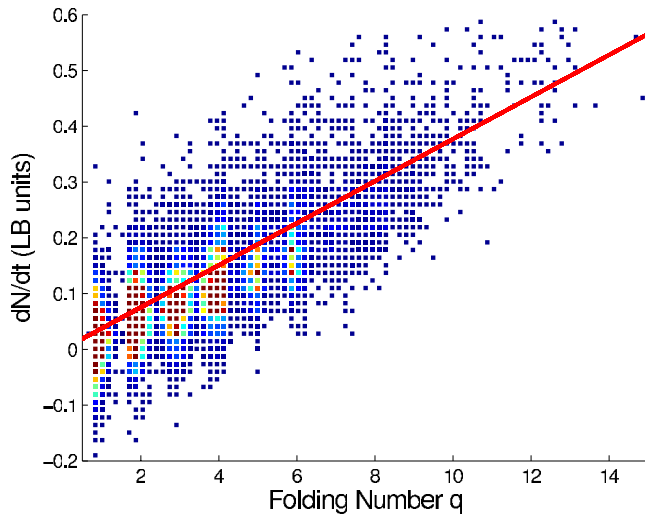


FIG. 4. (Color online) Scatter plot illustrating the correlation between the folding number q and the rate of translocating monomers dN/dt for the wide pore ($d_p=9$) and long polymer ($N=8000$) case. Colors indicate the density of points [blue (dark gray): low; red (light gray): high]; the straight line is the best linear fit.

$$N = \int_0^\tau \frac{dN}{dt} dt = K_N \int_0^\tau N_{\text{res}}(t) dt, \quad (1)$$

where we have used the fact that dN/dt and N_{res} are linearly correlated with a constant of proportionality K_N . Next, we write $N_{\text{res}}(t) = q(t)N_{\text{res},1}$, where the subscript 1 stands for the single-file ($q=1$) limit of the residence number. Equation (1) then leads to $N = K_N N_{\text{res},1} \bar{q}_N \tau$, where \bar{q}_N is the time-averaged value of q . By averaging over all realizations, we obtain

$$\tau_{\text{mf}}(N) \sim \frac{N}{N_{\text{res},1} \langle K_N \rangle \langle \bar{q}_N \rangle} \equiv \frac{\tau_1(N)}{\langle \bar{q}_N \rangle}, \quad (2)$$

where angular brackets stand for ensemble averaging, $\tau_{\text{mf}}(N)$ is the multifile translocation time, and we have defined

$\tau_1(N) \equiv (N/N_{\text{res},1})(1/\langle K_N \rangle)$; note that the dependence of $\langle K_N \rangle$ on N is responsible for the nonlinearity of $\tau_1(N)$. The simulation data show that the average $\langle \bar{q}_N \rangle$ remains approximately constant ~ 1.2 , for $N < 1000$, and then begins growing, reaching ~ 2.6 for $N=8000$. Therefore, we conclude that the departure of the translocation time from a power law at large N is mainly due to the increase of $\langle \bar{q}_N \rangle$ with polymer length, for $N > 1000$. This, in turn, results from the shift of the probability distribution of the translocation time toward higher q values as N is increased. For all lengths N considered here, the time average $\langle \bar{q}_N \rangle$ remains below 3, because the states $q=1$ and 2 continue to be the most populated ones for both pore diameters $d_p=5$ and 9. We have also checked that the high- q peaks have a sizeable effect only on moments $\langle q^p \rangle$ for $p \geq 5$. Since the average translocation time is only a first-order moment, the quantized peaks have little effect on it. This explains why the two pores, $d_p=5$ and 9, show similar dependence of $\langle \bar{q}_N \rangle$ on N . As a self-consistency check, in Fig. 3 we show the average translocation time for the case $d_p=9$, and compare it to the single-exponent estimate $\tau_1(N) \sim N^{1.31}$ and the compensated multifile translocation time, $\tau_{\text{mf}} = \tau_1(N)/\langle \bar{q}_N \rangle$. The reasonable match of τ_{mf} with the data supports the idea that the speed-up of the longest chains can be attributed to the spectral shift of the folding number q .

Finally, we note that analyzing the in-pore conformation versus q is an important aspect of multifile translocation. In the present Rapid Communication, we focused on how translocation, and the accompanying single-file out-of-pore hydrodynamics, is modulated by the population of the in-pore states, but we have not analyzed in detail the in-pore conformations, which will be addressed in future work.

S.M. and M.B. acknowledge support by Harvard's Initiative in Innovative Computing. Computational resources were provided through the CyberInfrastructure Lab of the Harvard School of Engineering and Applied Sciences. We thank G. Lakatos for helpful comments.

-
- [1] H. Lodish *et al.*, *Molecular Cell Biology* (Freeman, New York, 1996).
- [2] J. J. Kasianowicz *et al.*, *Proc. Natl. Acad. Sci. U.S.A.* **93**, 13770 (1996).
- [3] A. Meller *et al.*, *Proc. Natl. Acad. Sci. U.S.A.* **97**, 1079 (2000).
- [4] C. Dekker, *Nat. Nanotechnol.* **2**, 209 (2007).
- [5] For a recent review of the field, see D. Branton *et al.*, *Nat. Nanotechnol.* **26**, 1 (2008).
- [6] J. Li *et al.*, *Nature Mater.* **2**, 611 (2003).
- [7] M. Bernaschi *et al.*, *Nano Lett.* **8**, 1115 (2008).
- [8] D. K. Lubensky and D. R. Nelson, *Biophys. J.* **77**, 1824 (1999).
- [9] A. J. Storm *et al.*, *Nano Lett.* **5**, 1193 (2005).
- [10] M. G. Fyta *et al.*, *Multiscale Model. Simul.* **5**, 1156 (2006).
- [11] C. Forrey and M. Muthukumar, *J. Chem. Phys.* **127**, 015102 (2007).
- [12] M. Fyta *et al.*, *Phys. Rev. E* **78**, 036704 (2008).
- [13] R. Benzi *et al.*, *Phys. Rep.* **222**, 145 (1992).
- [14] The Lennard-Jones parameters for bead-bead interactions are $\sigma_b=1.8$, $\epsilon_b=10^{-4}$, and cutoff distance 2.02; for bead-wall interactions, $\sigma_w=1.5$, $\epsilon_w=10^{-3}$, and cutoff distance 1.68.
- [15] Briefly, the bonds between adjacent beads are modeled by springs with constant $k=0.5$ and equilibrium length $b=1.2$; the solvent density is $\rho=1$, kinematic viscosity $\nu=0.1$ and friction coefficient $\gamma=0.1$ (all in LB units). With $\Delta x=42$ nm, b becomes equal to the persistence length of double-stranded DNA (50 nm).
- [16] A. J. Storm *et al.*, *Phys. Rev. E* **71**, 051903 (2005).
- [17] To be precise, $q_{\text{max}} = (d_p - \sigma_w)^2 / \sigma_b^2 = 17.36$ for $d_p=9$; but beads can get closer to each other than σ_b , and closer to the wall than σ_w , giving $q_{\text{max}} \sim 20$.
- [18] M. Zwolow and M. Di Ventra, *Rev. Mod. Phys.* **80**, 141 (2008).